Summer 8-18-2017

Creating Renewable Tunable Polymers from Hydroxymethylfurfural

Meredith C. Allen
University of Maine, meredith.allen@maine.edu

CREATING RENEWABLE TUNABLE POLYMERS FROM HYDROXYMETHYLFURFURAL

By

Meredith C. Allen

B.S. St. Lawrence University, 2013

A THESIS

Submitted in Partial Fulfillment of the

Requirements for the Degree of

Master of Science

(in Chemical Engineering)

The Graduate School

The University of Maine

August 2017

Advisory Committee:

Thomas J. Schwartz, Assistant Professor of Chemical Engineering, Advisor

Clayton Wheeler, Professor of Chemical Engineering

William DeSisto, Professor of Chemical Engineering

CREATING RENEWABLE TUNABLE POLYMERS FROM HYDROXYMETHYLFURFURAL

By Meredith C. Allen

Thesis Advisor: Dr. Thomas J. Schwartz

An Abstract of the Thesis Presented
in Partial Fulfillment of the Requirements for the
Degree of Master of Science
(in Chemical Engineering)
August 2017

This research addresses the conversion of 5-hydroxymethylfurfural (HMF) into a tunable polymer. HMF is a known cellulose derivative that can be acquired from biomass via hydrolysis of cellulose followed by isomerization and selective dehydration. The process considered here is being developed to create tunable polymers from HMF and involves several different steps, three of which are covered in this thesis. The first step, an etherification, is the reaction of HMF with an alcohol. This step is significant because the R-group from the alcohol is added to HMF and the resulting side-chain is carried over to the final polymer giving the polymer unique properties. Thus, by changing the reacting alcohol in the first reaction the final polymer is changed. Upon evaluation of this step various catalysts were tested to identify what active site is needed as well as how the morphology of different catalysts with the previously determined site affect the reactivity. In addition, R-group identity was evaluated to determine if the alcohol used affects the reactivity of the catalyst. For this reaction, it was found that a Brønsted acid active site is needed and that the pore structure of β-Zeolite (BEA) aids the production of an ether product giving both a high production rate and high selectivity for this product. Another important

finding is that the identity of the R-group does not greatly affect the amount of ether product produced, suggesting a role of the catalyst in the stabilization of HMF.

The second step, not investigated here, is to oxidize the aldehyde group in HMF to create a carboxyl group in its place. The other two reactions investigated involve the hydrogenation of the furan ring followed by a ring-rearrangement which causes the ring to grow to a six-membered lactone, still maintaining the ether branch from the first step. These two processes were first combined to determine if a bifunctional acid-metal catalyst could perform both steps under the same conditions. After it was determined that the conditions would need to be changed between reactions they were performed separately. For both reactions, it was found that bifunctional catalyst consisting of palladium supported on β-Zeolite (Pd /BEA) was effective, and separate reaction conditions were then developed for each step. The final step, not examined here, is a ring-opening transesterification polymerization to form the final polyester product. All three reactions evaluated here were performed individually to evaluate catalysts and reaction conditions. The products of each reaction were analyzed using GC-MS, GC-FID and HPLC.

ACKNOWLEDGEMENTS

The author thanks the UMaine Vice President for Research for providing start-up funds for this work, the Forest Bioproducts Research Institute for analysis setup, and the UMaine Catalysis group: Thomas J. Schwartz, Mohammed Al-Gharrawi, Hussein Abdulrazzaq, and Jalal Tavana for moral support. The author would also like to thank Christopher Stewart, Aiden Crane, Logan Doucette, and Hamdi Sheikh for their help in the lab. In addition, the author would like to acknowledge the continued support of her family: Beth, Doug, Hannah, and Greg Allen as well as Mike Kahler.

TABLE OF CONTENTS

LIST OF TABLES

LIST OF FIGURES

LIST OF ABBREVIATIONS

HMF 5-Hydroxymethylfurfural

Pd ..... Palladium

BEA ..... β-zeolite

Pd/BEA ..... Palladium-supported β-zeolite

MFI ZSM-5

FAU ..... Faujasite

MOR ..... Mordenite

HFCA ..... 5-hydroxymethyl-2-furancarboxylic acid

1. INTRODUCTION

1.1. Significance

In a day and age where society is looking toward renewable resources to replace oil-based ones to make all our products, biomass is at the forefront. Biomass, especially lignocellulosic biomass, is an attractive resource as it is renewable, biocompatible, biodegradable, and readily available worldwide from forestry, agricultural and agro-industrial wastes.[1,2] Much of the biomass research completed up to this point deals with the creation of renewable fuels or fuel additives from cellulose.[3] The current global market poses an issue for this research because current prices for oil are low and there is an increase in production (see Figure 1.1) ensuring its role as the more financially viable option.[4] This circumstance has triggered a shift in the target for renewable research to high-value chemicals.[5] Another factor which makes this path more practical is the use of lower-carbon-number species (C_1-C_3) in the oil industry forcing the development of new methods to make higher-carbon-number chemicals. This need for the oil industry to develop new processes increases the opportunity for higher-carbon-number biomass species to be used instead of fossil-based resources.[6] In a review by Isikgora and Becer, 16 platform chemicals derived from the lignocellulosic sugars are mapped out to well over 150 chemicals that have already been synthesized from these molecules.[7] One noteworthy molecule shown by these authors is lactic acid; this chemical has been polymerized into polylactic acid (PLA). PLA has been used as a biodegradable and compostable alternative in the packaging, agriculture, automobile, electronics, and textile industries.[8] The use of PLA is promising, but its low glass transition temperature and its brittleness restrict it as a replacement material for oil-based thermoplastics like PET.[9] Current work with PLA pursues ways to improve its performance while other work looks for alternative polymers that are more

adaptable. This study considers a process of deriving tunable polymers from biomass. Some of the characteristics of these polymers which could be tuned include barrier permeability, strength, pressure tolerance, and transparency, all leading toward a more appealing alternative for oil-based plastics. The work here deals with the development of a process that begins with 5-hydroxymethylfurfural (HMF) and ends with a tunable polymer that could offer a variety of potential properties and functions. The development of this process could be a significant step forward in the transition to renewable, biobased chemicals.

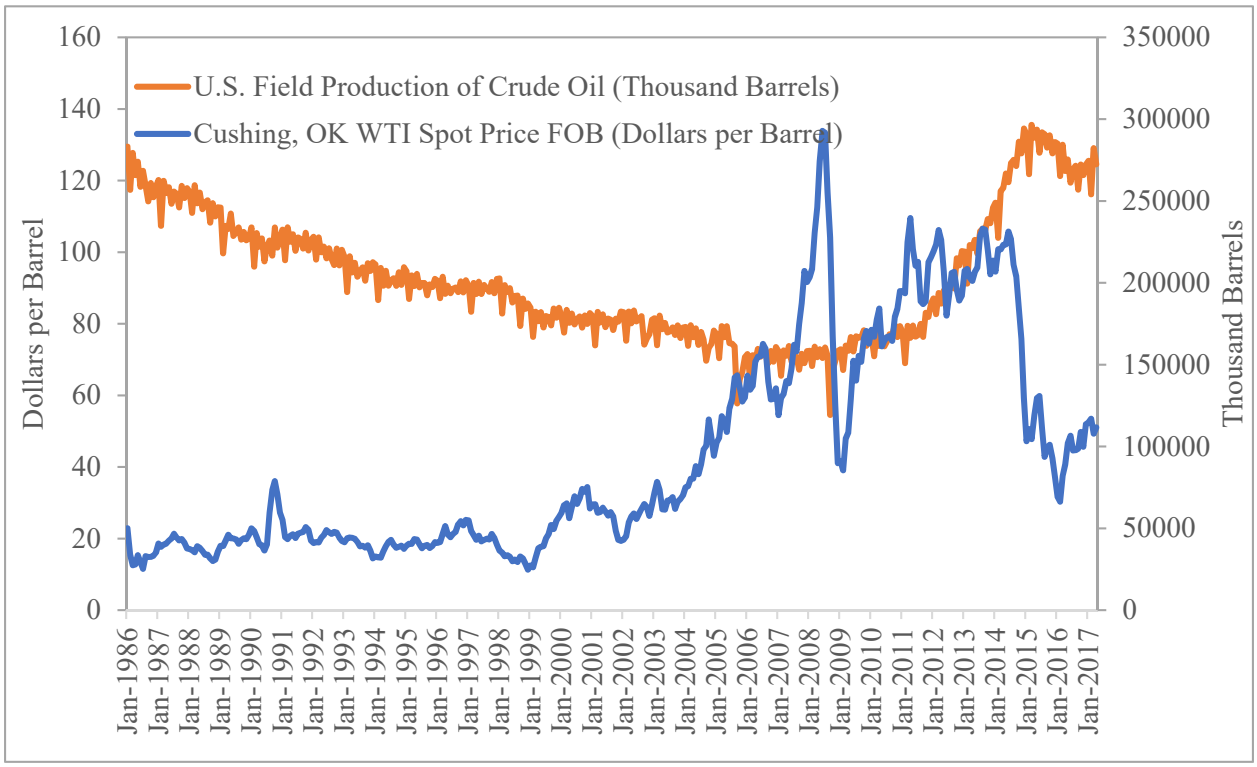

Figure 1.1: Production of Crude Oil and Price of Crude Oil. Data from the U.S. Energy Information Administration.[4]

1.2. HMF

This study seeks to start with a biomass derived chemical, HMF, which can be acquired through a series of reactions starting with cellulose (see Figure 1.2). The increase in interest in HMF originated with a report from the U.S. Department of Energy in which it was mentioned as a top 10 building block chemical from biomass.[10] At this point in time the production of HMF

has been taken on from three different approaches outlined in a review in *Green Chemistry*.[11] The first approach was to use high boiling point solvents and ionic liquids. As an example, Tong et. al. achieved a 72.3% yield of HMF with 87.2% using 7.5 mol% $[NMP]^+$ $[CH3\ SO3]^-$ (an ionic liquid) in dimethyl sulfoxide.[12] This approach showed promising results but the main drawback was the expensive separation of HMF from these high boiling point solvents. The second approach was to use water as the solvent. With this approach, one example of these reactions was performed using niobic acid and niobium phosphate in water with this reaction a selectivity of HMF of about 30% was achieved but it was found that these catalysts can deactivate quickly.[13] Low selectivity for these reactions is thought to be due to the degradation of HMF in the aqueous solution.[14] With advantages and drawbacks to using either a high boiling point solvent, high selectivity but difficult separation, or water, side reactions but easier to recover, a third approach was taken. This third approach uses a biphasic system in which water (or a modified solution typically with sodium chloride) is used for the catalytic solvent and then once HMF is formed it drops into an organic phase where it is unable to form degradation products. Within this research many organic phases, modifiers for the aqueous phase, catalysts, and ratios of aqueous to organic phase have been examined. The solvents used, especially the extracting organic phase used has been varied depending on the final purpose of the HMF. For example when no further separation is needed, high boiling point solvents and ionic liquids are favored, when HMF needs to be extracted other organic solvents such as tetrahydrofuran and 1-butanol have been used.[15] With additional research HMF is expected to become a more economically feasible and reliable feedstock as its uses as a platform for high-value chemicals. Twelve chemicals derived from HMF are given by Isikgora and Becer in their review from 2015.[7] This

work shows that HMF is a reasonable feedstock for this process. And therefore, it is from HMF that this work starts, with the goal of ending at a tunable polymer.

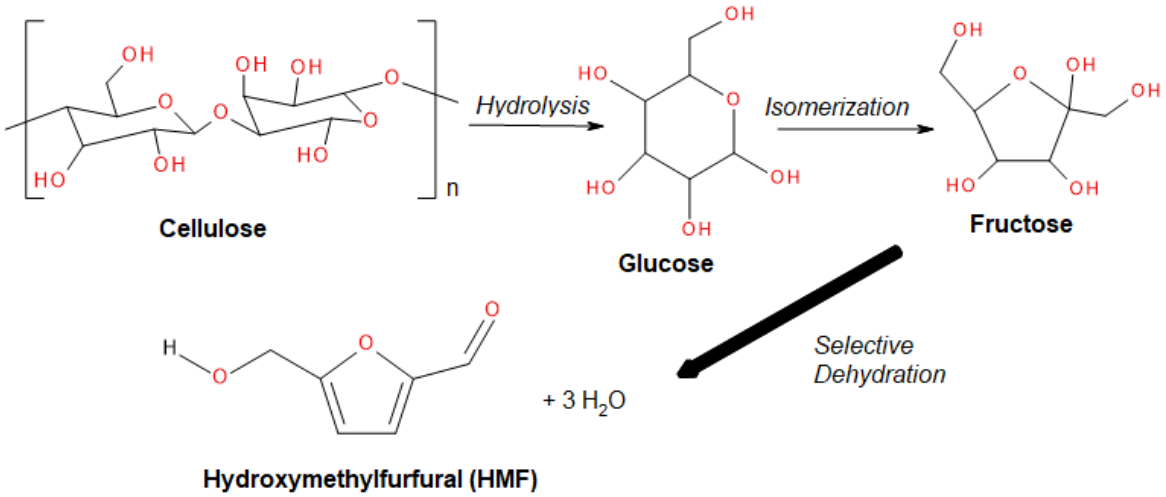

Figure 1.2: Reaction Scheme to Create 5-Hydoxymethylfurfural from Cellulose.

1.3. Overall Reaction Scheme

For this research, the focus is taking HMF and developing several reactions that follow to obtain a tunable polymer, as shown in Figure 1.3. The full procedure includes five major reactions, three of which are covered in this study. Reaction 1 is the etherification of HMF by reacting it with an alcohol over a catalyst. The alcohol will be added to HMF by an addition to the R-group of the alcohol to the OH branch of HMF and the loss of a water molecule. Reaction 2, not covered here, involves the oxidation of the ketone branch, converting it into a carboxylic acid. It is suspected that the same method used in a different study in which HMF was oxidized to produce 5-hydroxymethyl-2-furancarboxylic acid (HFCA) would still work for the ether modified products obtained in reaction one.[16] In the literature, it was found that reactions catalyzed with gold supported on carbon or gold supported on titanium oxide were able to produce HFCA without continuing on to other byproducts. Once the oxidation is complete, the third reaction saturates the furan ring in furfural. The fourth reaction involves the rearrangement of the saturated ring into lactone. The fifth and final step is to create the monomer structure; to

do this the bond between the oxygen and its neighboring ketone is severed in a ring-opening transesterification polymerization. With this final step, the monomers are also linked together, forming the fully tuned polymer. This final step will be performed by Dr. William Gramlich in the chemistry department at the University of Maine.

This study specifically focuses on the viability and development of steps one, three, and four. The first reaction was developed by determining: the active site for this reaction, the role of catalyst morphology, and the effect of R-group identity has on the rate and selectivity of this reaction. The third and fourth reactions, hydrogenation and ring rearrangement, were first studied together but upon further investigation were performed separately. Covered here are all the findings for these three reactions as well as methods and conclusions for each.

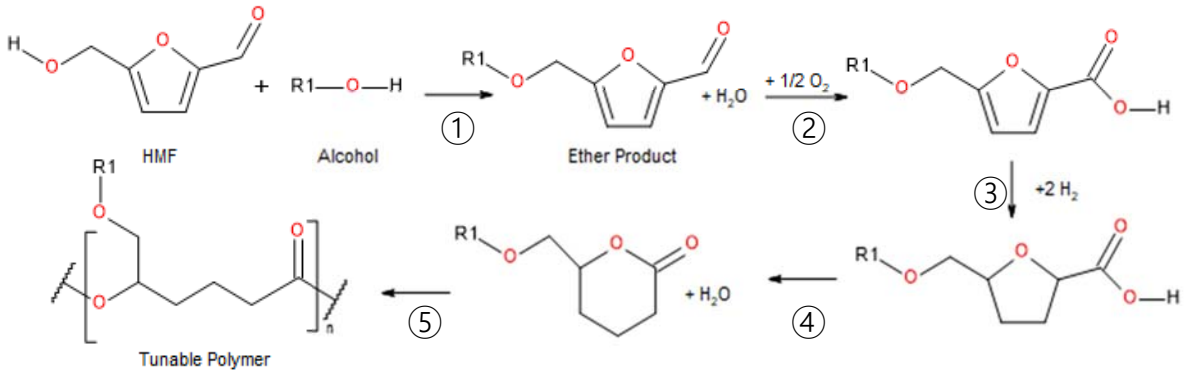

Figure 1.3 Overall Reaction Scheme. Starting with 5-hydroxymethylfurfural and ending with the polymer.

1.4 What is Covered Here

The information covered here will include the materials and methods used for this work in Chapter 2. The results and discussion for catalyst and reaction condition development for the first reaction (etherification) in Chapter 3, and the third (hydrogenation) and fourth (ring rearrangement) reactions both in Chapter 4. This work will also include what these results mean for the lager purpose of this work as well as suggestions for future directions in Chapter 5.

2. MATERIALS AND METHODS

2.1 Etherification Catalyst Preparation

2.1.1 Catalyst Preparation

The zeolite catalysts β-Zeolite (BEA) with SiO_2:Al_2O_3 of 25 (ammonium form), 38 (ammonium form), and 300 (hydrogen form) (BEA-25, BEA-38, and BEA-300, respectively) were acquired from Zeolyst International. ZSM-5 in its ammonium form (MFI, SiO_2:Al_2O_3=23), mordenite in its ammonium form (MOR, SiO_2:Al_2O_3=20), and faujasite in its ammonium form (FAU, SiO_2:Al_2O_3=5.1) were also acquired from Zeolyst International. Amorphous SiO_2-Al_2O_3, (Davicat 3113, ASA, SiO_2:Al_2O_3=5.1) was acquired from Grace Davison. γ-alumina was acquired from Alfa-Aesar. These catalysts were then calcined in air (Matheson, breathing air) at 550 °C for 1 hour (3-hour ramp at rate of 3 °C/min). The resulting catalysts were crushed and sieved resulting in 180 μm particles. Amberlyst-15 in its hydrogen from (Sigma Aldrich) was washed in DI water and dried overnight in an oven at 110°C. The washed Amberlyst-15 as well as tungsten (VI) oxide (WO_3, Fluka) and hydrotalcite (Sigma Aldrich) were crushed and sieved to the 180 μm.

2.1.2 Etherification Reactions

Ring rearrangement reactions were performed in thick-walled glass batch reactors (Alltech, 10mL) equipped with triangle stirrers and sealed with PTFE liners (Qorpac) in plastic caps (Qorpac). 0.05 g of HMF (Acros Organics, 98%) along with 0.05 g of catalyst was used for all reactions as well as 4 g of 1:3 (g:g) alcohol in water for the solvent and excess reactant. Alcohols used include ethanol (Acros Organics, 99.5+%), butanol (Sigma, ≥99.4%), phenol (Fisher, 91%), and cyclohexanol (Fisher, reagent grade). Initially, catalysts were evaluated using ethanol only. Reaction temperatures were maintained at 160 °C in a stirring oil bath and reaction

times ranged from 15 minutes to 96 hours to achieve the desired HMF conversions. Selectivity was measured at 70-80% HMF conversion and initial rates were measured at 10-15% HMF conversion. When comparing results of multiple different alcohol etherification reactions were run for 15 min, 45 min, 1.5 hr, 2.5 hr, and 4 hr, and the products were analyzed for each separate reaction using a gas chromatograph equipped with a flame ionization detector (GC-FID).

2.1.3 Analysis

Reaction products were quantified using a Shimadzu GC-2010 with an APC-2010 FID detector. Separation was achieved using an Agilent 122-1334UI column (30 m x 0.025 mm, 1.40 μm). Helium (Matheson, grade 5.0) with a linear velocity of 35 cm/s was used as the carrier gas.

Components were identified and quantified using standards made for HMF (Acros Organics, 98%), 5-(Ethoxymethyl)furan-2-carboxaldehyde (EMF, Sigma Aldrich, 97%), ethanol (Acros Organics, 99.5^{+}%), butanol (Sigma, ≥99.4%), phenol (Fisher, 91%), and cyclohexanol (Fisher, reagent grade).

2.2 Hydrogenation and Ring Rearrangement

2.2.1 Catalyst Preparation

Palladium supported on beta zeolite (Pd/BEA) was prepared for both the hydrogenation and ring rearrangement reaction through the adaptation of an ion exchange method used by Gallastegi-Villa.[17] The ammonium form of BEA (SiO_2:Al_2O_3 = 25) zeolite was calcined in air (Matheson, breathing air) at 550 °C for 1 hour (3-hour ramp at rate of 3 °C/min). 0.21 g of tetraamminepalladium(II) nitrate solution (5.0 wt% Pd, Strem Chemical) was added per gram of calcined BEA to a 200 mL solution of DI water. The solution with the calcined catalyst was then heated and stirred at 65 °C for 24 hours to obtain a 0.37 wt% Pd loading. This solution was then

filtered, washed twice with DI water, and dried overnight in an oven at 110 °C. The dry catalyst was then calcined in air at 500 °C for 3 hours (8-hour ramp at rate of 1 °C/min). Once cool, the catalyst was reduced in hydrogen (Matheson, grade 4.5) at 260 °C for 4 hours (4-hour ramp at rate of 1 °C/min). The resulting catalyst was crushed and sieved resulting in 180 μm particles. The catalyst was used in both hydrogenation and ring rearrangement reactions. The ammonium forms of BEA (SiO_2:Al_2O_3=25) and ZSM-5 (MFI, SiO_2:Al_2O_3=23) catalysts were purchased from Zeolyst International and used for comparison. These were calcined in air (Matheson, breathing air) at 550 °C for 1 hour (3-hour ramp at rate of 3 °C/min). The resulting catalysts were similarly crushed and sieved resulting in 180 μm particles.

2.2.2 Hydrogenation Reactions

Hydrogenation reactions were performed in a 25mL Parr batch reactor with a hydrogen pressure of 500 psi (Matheson, grade 4.5). For each reaction 15 g of a 5 wt% solution of 2-furoic acid (Acros Organics, 98%) in tetrahydrofuran (Fisher, 99+%) was used with 0.05g of catalyst. A ramp rate of 5 °C/min was used to bring the reaction up to 120 °C where it was held for 4 hours with 500 rpm stirring. Temperature was controlled with a Parr 4857 process controller and a Parr 4875 power controller. Once complete a sample was taken and filtered with a 0.45 μm syringe filter. Samples were then analyzed via high performance liquid chromatrography (HPLC).

2.2.3 Ring Rearrangement Reactions

Ring rearrangement reactions were performed in thick-walled glass batch reactors (Alltech, 10 mL) equipped with triangle stirrers were sealed with PTFE liners (Qorpac) in plastic caps (Qorpac). A temperature of 100 °C was maintained with a stirring oil bath (400 rpm) for 4 hours although both the time and temperature were varied from 1-24 hours and 80-180 °C

respectively. 0.05 g of Pd/BEA catalyst was used with 4 g of tetrahydropyran (Alfa Aesar, 98+%) and 0.075 g of tetrahydro-2-furoic acid (Acros Organics, 99+%). Once complete a sample was taken and filtered with 0.45μm syringe filter. Samples were then analyzed via gas chromatography-mass spectrometry (GC-MS).

2.2.4 Analysis

Reaction products for the hydrogenation reaction were analyzed using a Shimadzu HPLC (LC-20AD) with a RID-10A refractive index detector and an SPD-20AV UV/Vis detector. Samples were separated with an Aminex HPX-87H column (300 x 7.8 mm, 9 μm). A 5 mM solution of sulfuric acid (Fisher, 96.5%) in Milli-Q water was used as the mobile phase.

Reaction products for the ring rearrangement reaction were analyzed using a Shimadzu GC-MS (GC-2010 with a QP2010 mass spectrometer). Separation was achieved using a Restek RXI-5ms column (30 m x 0.25 mm, 0.25 μm). Helium (Matheson, grade 5.0) and Air (Matheson, grade 2.0) at a linear velocity of 36.1 cm/s were used as the carrier gases.

Standards for both instruments were made with 2-furoic acid (Acros Organics, 98%), tetrahydro-2-furoic acid (Acros Organics, 99+%) and δ-valerolactone (Alpha Aesar, 98%).

3. ETHERIFICATION REACTION

3.1. Etherification

3.1.1 Overview

Etherification is the first reaction of the overall processing scheme, and it is shown generally in Figure 3.1. In this reaction HMF is reacted with an alcohol forming the R-group which is carried through the rest of the reactions. This step is key as the R-group will give each polymer its distinct properties. The ability of a catalyst to work with different alcohols is paramount as the use of multiple catalysts would further complicate the reactor setup for this reaction. In addition, if the R-group affects the rate of reaction or prevents the formation of certain functionalization in the polymer this would reduce the versatility of the final polymer.

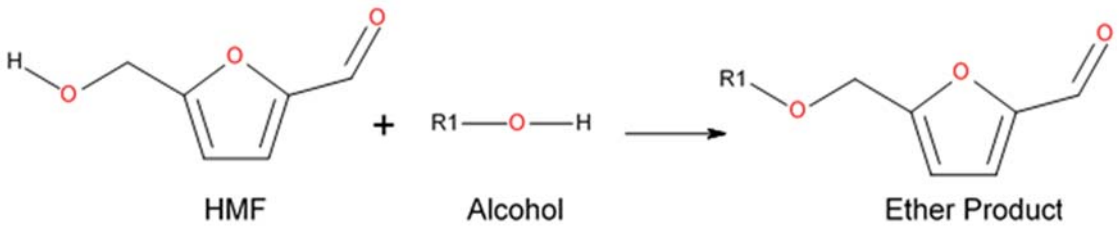

Figure 3.1: Etherification of 5-Hydroxymethylfurfural.

3.1.2 Previous Work

The etherification of HMF has been studied extensively in the past. Typically, past work has dealt with the use of ethanol to produce 5-(ethoxymethyl) furan-2-carbaldehyde (EMF) a component used in biodiesel. For these reactions, several different catalysts were used including: Amberlyst-131,[18] Zirconia supported on SBA-15,[19] and MCM-41.[19] Sn-BEA and HCl were used to perform a one pot reaction to create EMF from glucose.[18] Another study performed an etherification where HMF was reacted with tert-butanol to form 5-tert-butoxymethylfurfural, another component for biodiesel with H-BEA-25 (SiO_2:Al_2O_3=25).[20] All catalysts used in previous studies suggest acid sites are needed to perform this reaction but it is not entirely clear

if Brønsted sites are the only ones which can perform these reactions or if the presence of Lewis sites also influences this reaction.

In one study, the mechanism for this reaction was proposed. Balakrishnan et. al. suspected that the transition state for this reaction is a protonated HMF molecule.[21] If this is the case then reactions with a variety of R-groups should not greatly affect the formation of an ether product as the alcohol is not involved with the transition state.

There are concerns about unwanted byproducts for this reaction. The main concern is levulinic acid. From the literature, catalysts similar to those studied here were used in reactions to produce levulinic acid from furfuryl alcohol.[22] These authors found that, of the catalysts they tested, ZSM-5 produced the most levulinic acid, which was attributed to a morphology that allows for the production of levulinic acid while inhibiting furfuryl alcohol polymerization. Other catalysts tested such as BEA, MOR, and Amberlyst-15 also showed significant productions of this byproduct.

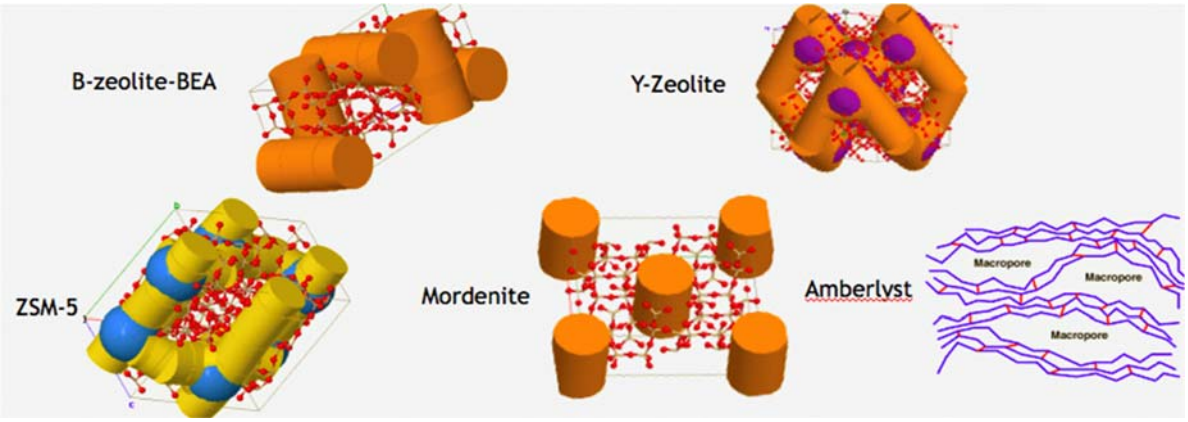

Figure 3.2: Morphologies of Acid Catalysts.[30]

Catalyst morphology itself can provide a way to screen products and reactants by allowing certain ones access to active sites, potentially providing additional support to intermediates, or changing the acid strength of sites.[23] The variation amongst the acid catalysts

here in architecture as well as pore size could greatly affect their reactivity. The different morphologies of these catalysts are shown in Figure 3.2.

3.2 Results and Discussion

3.2.1 High HMF Conversion

The first parameter used to compare catalysts was the selectivity, Equation 3.1, for the ether product, EMF. This number demonstrates how efficient the catalyst is at producing the desired ether product. All catalysts were run to a conversion of HMF between 70 and 80% to compare their selectivities. Figure 3.3 shows the selectivities obtained at high conversion for all the catalysts used. The first major observation from this work is that almost all the catalysts which have Brønsted sites, except for amorphous SiO_2-Al_2O_3, were able to achieve the high conversion needed to compare selectivities, whereas catalysts without these sites were inactive. This suggests that a Brønsted site is needed to perform this etherification reaction. It can also be seen that all BEA catalysts (SiO_2:Al_2O_3 =25, 38, and 200) were the most selective toward EMF with the highest selectivity (96%) observed for BEA-25. This is a potential consequence of the BEA structure and may be related to what was seen by Sarazen.[23] This suggests that a characteristic of BEA is allowing the catalyst to form EMF itself more readily perhaps by stabilizing a transition state or preventing the formation of unwanted side products such as levulinic acid. The cage structures of MFI, MOR, and FAU may not be able to facilitate this reaction in the same way and therefore cause lower EMF selectivities.

Levulinic acid was not observed as a byproduct for any of these reactions. It is suspected that the confinement effects of catalysts such as BEA prohibited its formation. Another hypothesis is that the solvent used here, 1:3 water: alcohol, did not have the same effect as the water and aprotic solvent used by Mellmer.[22]

$$Selectivity\ (\%) = \frac{(final\ mol\ of\ EMF)}{(initial\ mol\ of\ HMF - final\ mol\ of\ HMF)} * 100$$ Equation 3.1

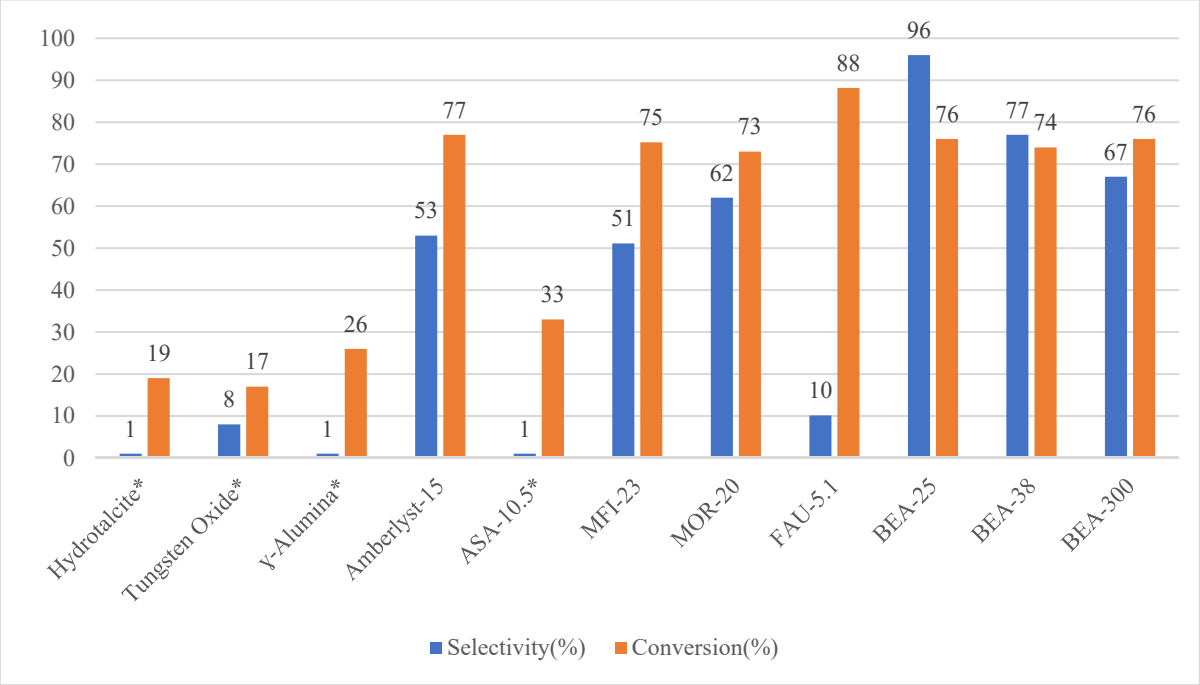

Figure 3.3: Selectivity for Different Catalysts. Selectivity is based on the amount of HMF converted to EMF at 70-80% conversion. *No reactions performed had 70-80% conversion at 433K

3.2.2 Low HMF Conversion

All catalysts were subsequently run to 10-15% HMF conversion to compare their EMF production rates (Figure 3.4). From these results, there are two catalysts that stand out with the highest production rates; Amberlyst-15 and BEA-25. The next nearest catalyst, BEA-38, has a production rate that is about half that of BEA-25 which should be expected since it has less Al_2O_3 and therefore fewer Brønsted active sites. To look more into the very high production rate for Amberlyst-15 and the low selectivity of Amberlyst-15 a plot of selectivity over time was created (Figure 3.5). This figure shows that as more HMF is converted the selectivity for EMF decreases. This explains that although a fast-initial rate is observed and a lot of EMF is produced,

over time the product is undergoing side reactions and a high selectivity is not observed for high conversion with this catalyst.

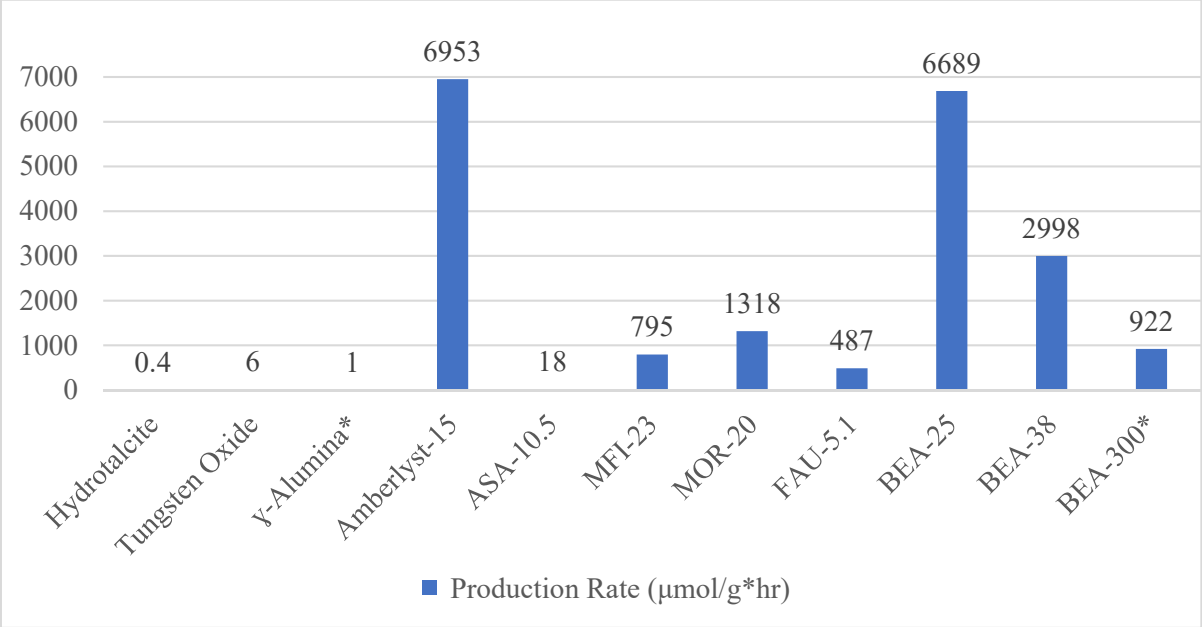

Figure 3.4: Production Rates for Different Catalysts. Production rates are the amount of EMF produced per gram of catalyst per hour at 10-15% conversion. *No reaction in 10-15% conversion was achieved at 433K

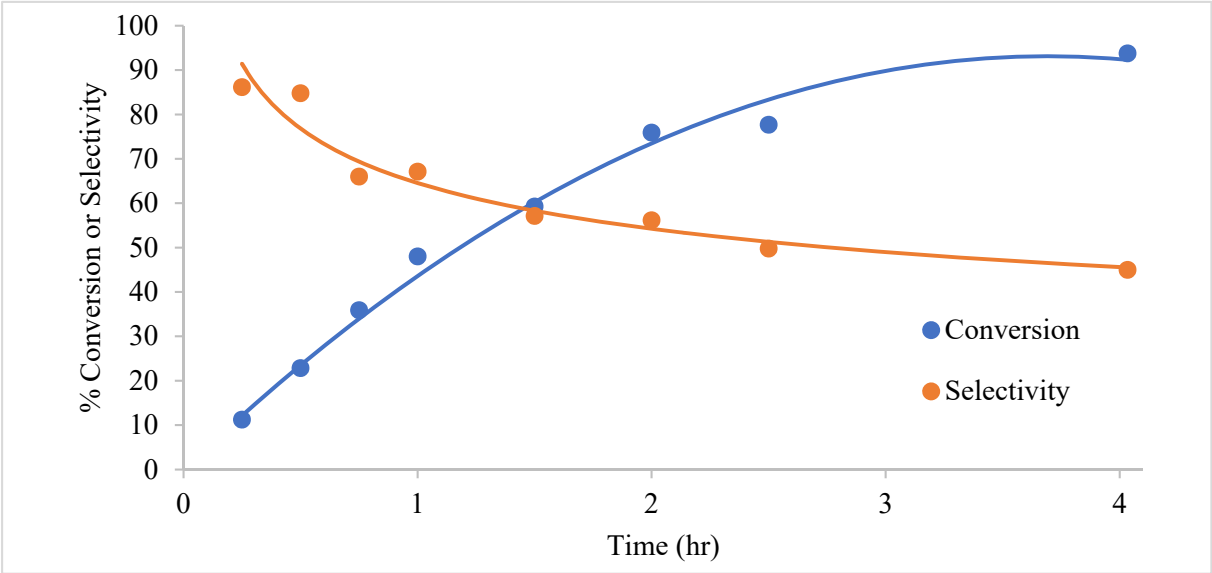

Figure 3.5: Selectivity and Conversion for Amberlyst-15.

Since it was already demonstrated that the non-Brønsted catalysts are inactive the low production rates for these catalysts are as expected. Unexpectedly amorphous SiO_2-Al_2O_3 appears to be inactive for this reaction. It might be expected that since this catalyst has Brønsted active sites that are accessible on the surface that a reaction would occur more readily. These results then further suggest that in addition to Brønsted sites the pore structure of BEA helps to stabilize a reaction intermediate.

3.2.3 SiO_2:Al_2O_3 and Rate

One might expect that the more Brønsted sites would result in higher production rates but, this expected trend is not observed for all zeolite morphologies. To better demonstrate this the production rate of these catalysts was graphed as a function of the SiO_2:Al_2O_3 ratio (Figure 3.6). Here we see that although many of the catalysts tested have more Al_2O_3 and therefore more Brønsted sites this does not necessarily result in a faster reaction rate. We see that MFI, FAU, ASA, and MOR all have low reaction rates and that these rates increase as the number of Brønsted sites are reduced. It is also seen that the three BEA catalysts follow a different trend where the rate decreases the SiO_2:Al_2O_3 ratio is increased. The rate of decrease is also smaller than expected given the dramatic reduction of sites especially from SiO_2:Al_2O_3 ratio of 25 to 300 which has very few Brønsted sites, possibly due to the inaccessibility of some of the sites in higher ratio species. From this figure, it can be seen clearly that SiO_2:Al_2O_3 is not the best way to explain the trend in reaction rate for all the zeolites tested as they follow two different trends, one with BEA zeolite and one for non-BEA zeolites.

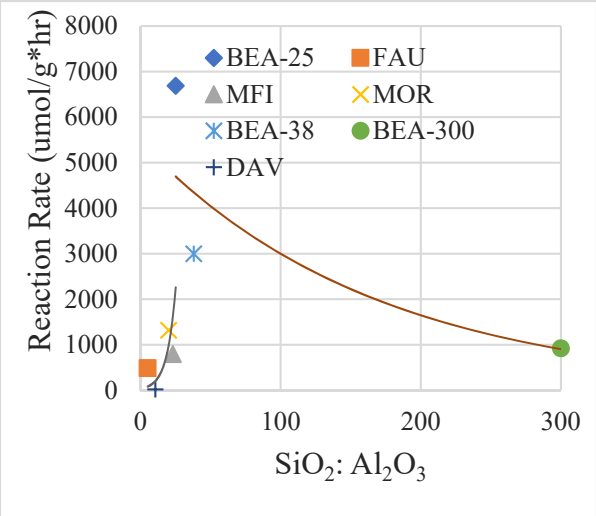

Figure 3.6: Comparing Reaction Rate and SiO_2:Al_2O_3 ratios for Zeolites. *BEA-300 had 17% conversion

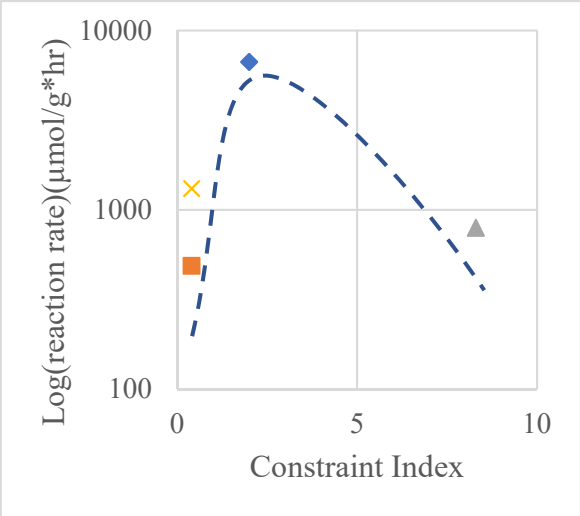

Figure 3.7: Reaction Rate and Constraint Index for Zeolites.

3.2.4 Constraint Index and Rate

Another way in which zeolite catalysts are compared is the constraint index.[24] This is commonly used in petroleum refining and is a measure of the ratio of the cracking rates of hexane and 3-methylpentane (Equation 3.2). Therefore, this index is an indication of shape selectivity of the catalyst. For comparison values from the literature were used to compare the production rates for the zeolite catalysts.[25] We can see in Figure 3.7 that a volcano plot is formed in which the maximum rate occurs at a constraint index of approximately 2, and we see that the rate drops off on either side. From the literature, we can also find that the kinetic diameter, the largest diameter of the molecule assuming it is spherical, of HMF is 6.2 Å.[25] From looking at Table 3.1 the pore size of MFI runs smaller than this suggesting that the morphology of the zeolite does not allow sufficient HMF to enter. Looking at FAU the diameter of these pores is large enough for HMF to enter; however, this does not have a positive impact on the rate or selectivity for this reaction. BEA has a pore size which is nearly identical to that of HMF signifying that the heightened reaction rate may be the cause of the increased production rate.

This then suggests that the specific structure of BEA may stabilize the transition state for etherification, assuming high concentration of the transition state on the surface, or, more likely, prevent the formation of byproducts resulting in greater selectivity for the EMF product.

$$Constraint\ Index = \frac{log\ (rate_{n-C6\ conv})}{log\ (rate_{3-MP\ conv})} \qquad \text{Equation 3.2}$$

Table 3.1: Zeolite Characteristics. Constraint index from Jae [25],Pore size and internal pore space from IZA Structure Commission [31]

Zeolite	SiO_2:Al_2O_3	Pore Size (Å)	Internal Pore Space (Å)	Constraint Index
BEA	25, 38, 300	6.6x6.7, 5.6x5.6	6.68	0.6-2.0
MFI	23	5.1x5.5, 5.3x5.6	6.36	6.9
FAU	5.1	7.4x7.4	11.24	0.4
MOR	20	6.5x7, 2.6x5.7	6.7	0.4

3.2.5 Varying the R-group

The next portion of this study looks at this reaction using different alcohols resulting in different R-groups compatibility for the tunable polymer. To test the versatility of BEA-25, several different alcohols with varying shapes, sizes, and electronic structures were used: ethanol, butanol, cyclohexanol, and phenol. Reactions for each alcohol were conducted for 15 min, 45 min, 1.5 hr, 2.5 hr, and 4 hr were analyzed for the ether product concentration. From the results shown in Figure 3.8 it can be inferred that the type of alcohol used, and thus the R-group added to HMF, does not greatly influence either the etherification rate or the selectivity to the ether product. This suggests that the increase in production by BEA seen earlier is due to the catalyst stabilizing a transition state that does not include the alcohol, suggesting an S_N1 mechanism in which the rate controlling step involves a protonated HMF molecule. This

suggests the mechanism shown in Figure 3.9, where the second step is rate-controlling, which is also consistent with the results found by Balakrishnan.[21]

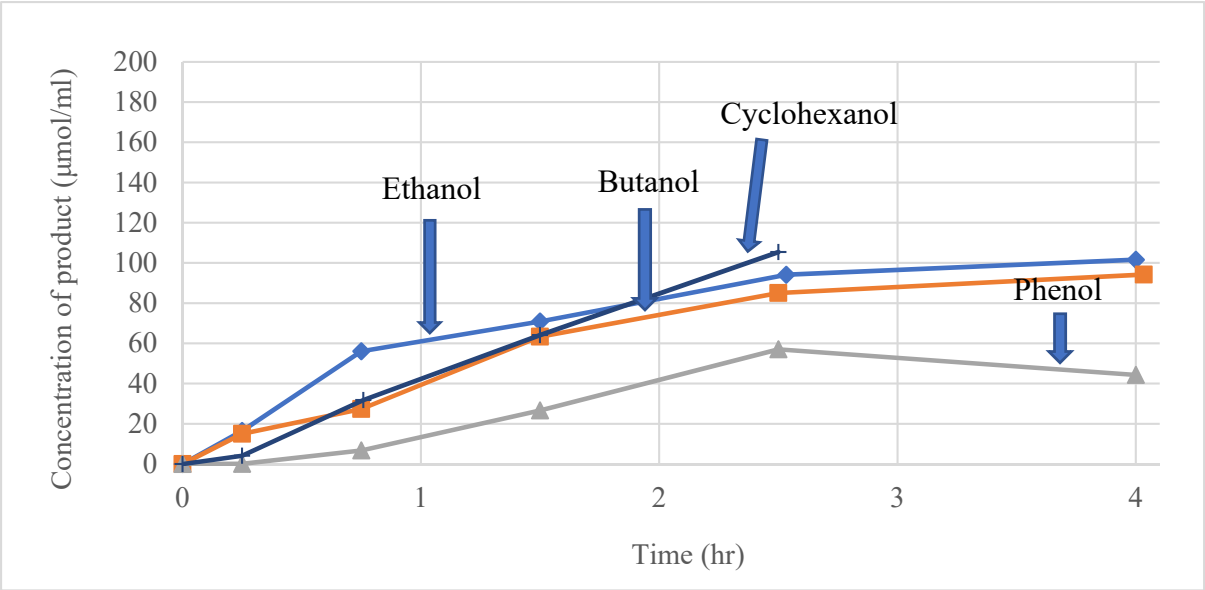

Figure 3.8: BEA-25 with Different Alcohols. Batch Reactor 7:10 catalyst: HMF ratio 4 g of 1:3 alcohol water solution 433 K.

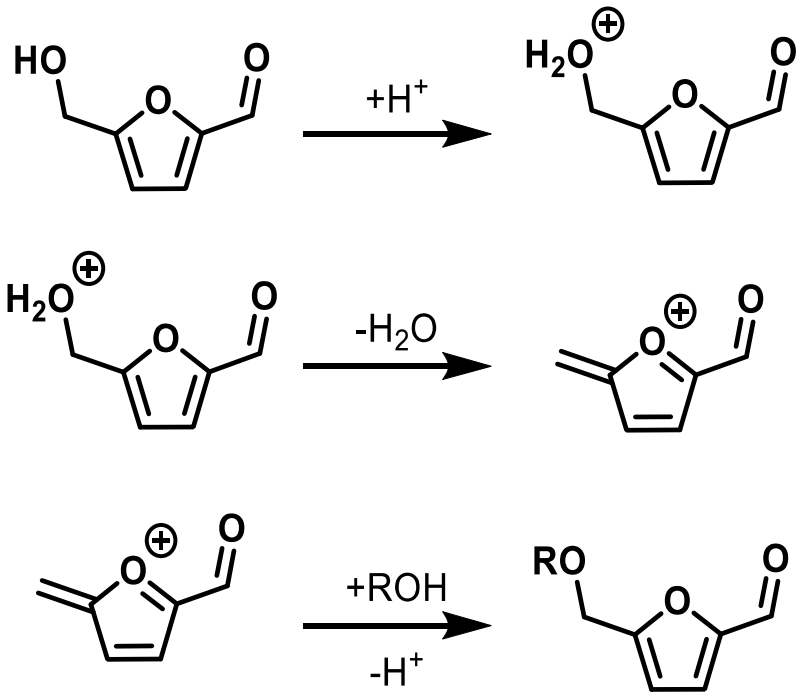

Figure 3.9: Proposed $S_N1$mechanism for HMF etherification.

3.3 Conclusion

This study involved the development of a catalyst that would effectively perform the etherification of HMF with several different alcohols. From this work, it has been determined that a Brønsted acid site is needed to perform this reaction. This was demonstrated by the inactivity of all catalysts tested that did not possess such a site as well as the generally high activity for those that do. A second result is that BEA-25 seems to be the most effective catalyst because it has both a high reaction rate as well as a high selectivity for EMF. From the comparison of rate with the constraint index it can be inferred that this high productivity and selectivity are most likely due to the compatibility between HMF and the pores of BEA zeolite. Finally, based on the ability to use a variety of alcohols it was found that identity of the R-group does not appear to have a significant effect on the amount of ether product produced. Therefore, it is suspected that the transition state for the rate determining step involves HMF and not the alcohol.

4. HYDROGENATION AND RING REARRANGEMENT

4.1 Hydrogenation and Ring Rearrangement

4.1.1 Overview

This reaction is one in which the furan ring is saturated and then rearranged to form a lactone ring. The reaction as it would be in this scenario is shown in Figure 4.1. To test catalyst viability this reaction was first investigated using a less-substituted ring shown in Figure 4.2.

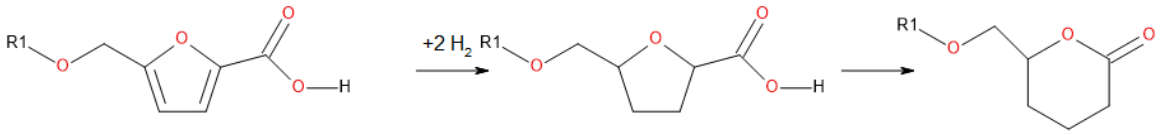

Figure 4.1: Hydrogenation and Ring Rearrangement Reaction.

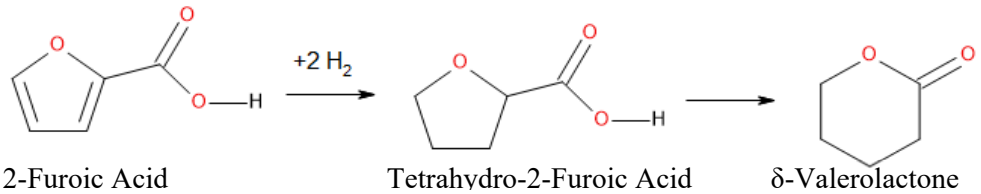

2-Furoic Acid Tetrahydro-2-Furoic Acid δ-Valerolactone

Figure 4.2: Modified Hydrogenation and Ring Rearrangement Reaction.

4.1.2 Previous Work

Although a reaction on these exact molecules has not yet been performed, Chia et. al were able to perform a similar ring reaction in a recent study with tetrahydrofurfuryl alcohol over a bifunctional rhodium rhenium (Rh-ReO_x/C) catalyst where the strong bond of the oxygen in hydroxyl groups on rhenium atoms associated with rhodium causes them to be acidic, making it likely that these groups are responsible for the proton donation which leads to the formation of carbenium ion transition states (Figure 4.4).[26] In a later study they determined that the Brønsted acidity was generated from the activation of water molecules over Re atoms on the surface of metallic Rh-Re particles.[27] With this bifunctional acid-metal catalyst they were able to open the reactant ring at the C-O bond with the most substituted carbon which is what the aforementioned

reaction needs to do. In addition, the catalyst needs to perform both the hydrogenation and ring rearrangement so palladium (Pd) was utilized for this as it is a common catalyst for hydrogenation. Based on this information a bifunctional palladium supported on β-Zeolite (Pd/BEA) catalyst was developed for this reaction. With this catalyst BEA is an acidic support, not an inert support like the carbon used by Chia, and Pd acts as the metal for the bifunctional catalyst. The proposed mechanism for the hydrogenation and ring rearrangement reaction is given in Figure 4.3. In this mechanism after the initial hydrogenation the ring rearrangement starts off with the furanic oxygen attacking a proton. This mechanism would suggest that both of these reactions can be completed with the proposed bifunctional Pd/BEA catalyst.

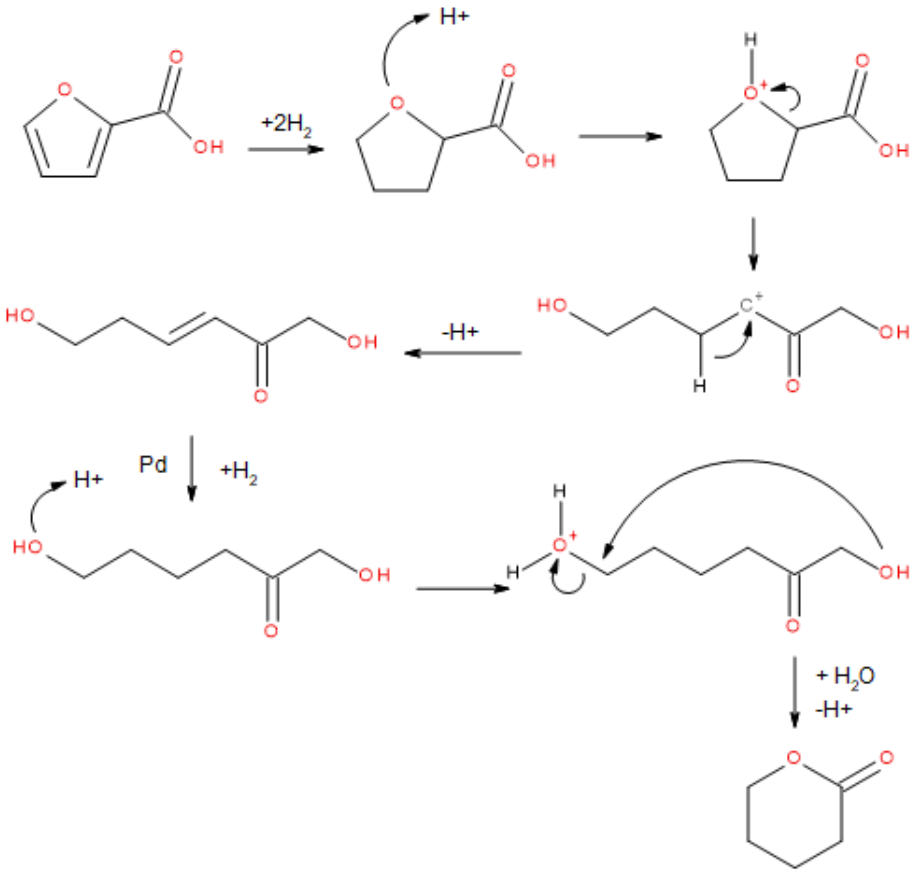

Figure 4.3: Proposed Reaction Mechanism for Hydrogenation and Ring Rearrangement.

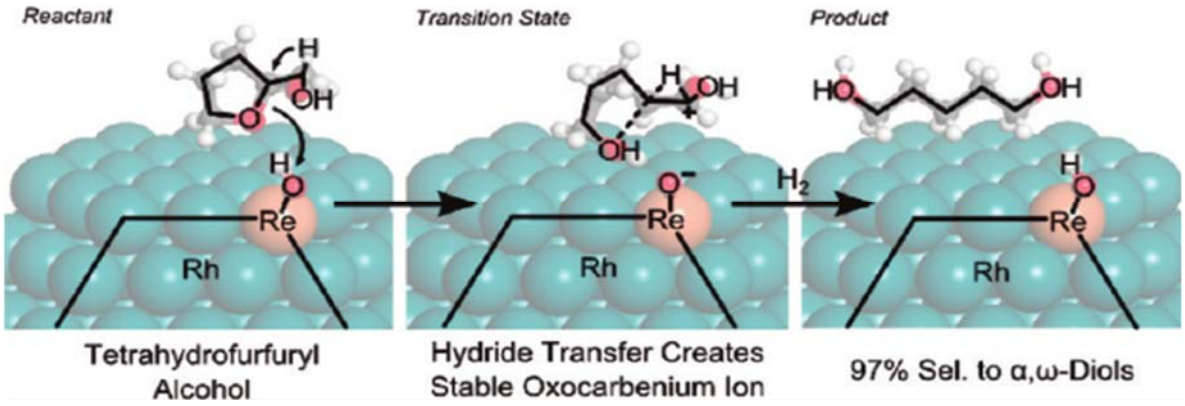

Figure 4.4: Mechanism for Ring Opening with Bifunctional Rh-ReO_x/C Catalyst.[26]

4.2 Results and Discussion

4.2.1 Hydrogenation and Ring Rearrangement

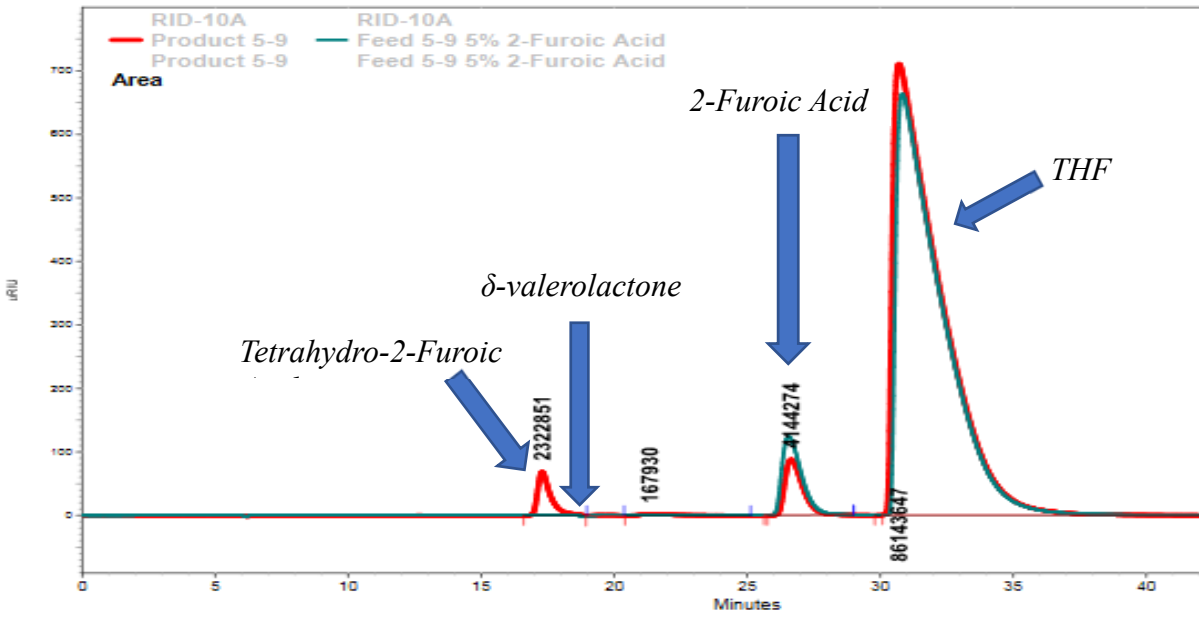

Figure 4.5: Hydrogenation and Ring Rearrangement Reaction. Feed (Teal) and Product (Red). 2-Furoic Acid in THF Time: 4 hr Temp: 120 °C Catalyst: Feed=30:1 Pd sub β-Zeolite 500 psi. H_2 Catalyst HPLC Results.

Initially reactions were run in a Parr reaction using 2-furoic acid as a model compound (Figure 4.2). One example of the initial HPLC results is shown in Figure 4.5. From those results, a reduction in the reactant concentration (peak at ~27 min) and we see that the hydrogenation product, tetrahydro-2-furioc acid, is formed (peak at 18 min). A peak for δ-valerolactone, the end product, was not observed (would occur as 19min) for any of these

reactions. From this, it was inferred that these reaction conditions work for the hydrogenation step but not for the ring rearrangement step.

4.2.2 Ring Rearrangement

4.2.2.1 Catalyst Validation

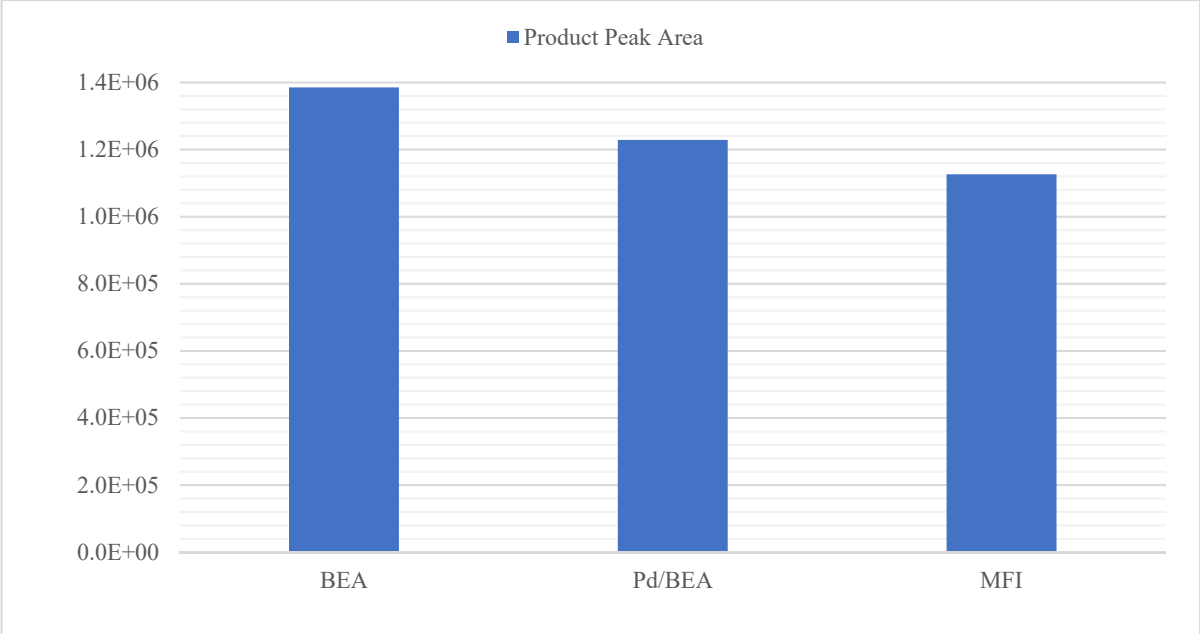

Figure 4.6: Catalyst Validation. Peak areas for δ-valerolactone with three different catalysts tested. Batch Reactor Tetrahydro-2-Furoic Acid in THP Reaction Time: 4 hr Catalyst: Reactant= 1:4 Reaction Temp: 120 °C GC-MS

To further investigate a reaction starting with tetrahydro-2-furoic acid was run to validate the activity of the catalyst, Pd/BEA. To do so reactions were performed in smaller batch reactors with the same temperature and time used in the Parr reactor. To compare catalyst reactivity of Pd/BEA, reactions were also run with BEA and another zeolite, MFI. These two alternative materials have the potential to catalyze this reaction, and neither of them have Pd, which can block the active sites that are suspected to be necessary for this reaction. Figure 4.6 first shows that all three catalysts are able produce the target product, δ-valerolactone, and second, that non-substituted BEA produced the most δ-valerolactone, followed by Pd supported on BeA, and finally MFI. The increase in δ-valerolactone production for BEA vs Pd/BEA is expected

because Pd can occupy the acid sites that are needed for this reaction. The decrease in production found with MFI is suspected to be due to transport limitations caused by the small pores of this catalyst.

4.2.2.2 Reaction Temperature

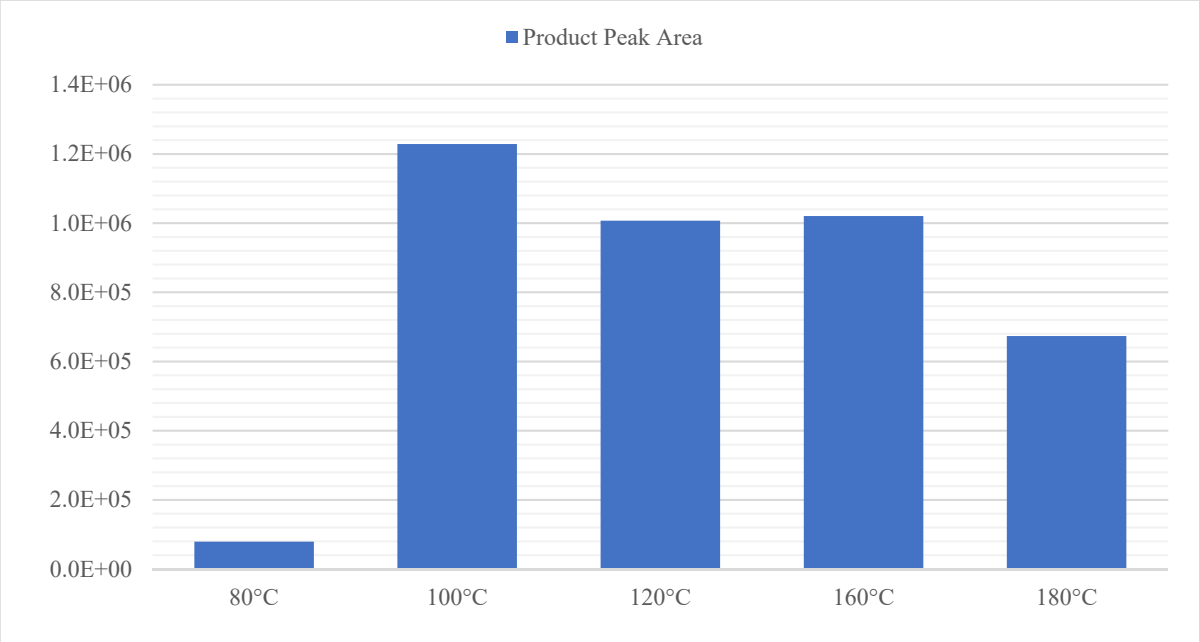

Figure 4.7: Reaction Temperature. Peak areas for δ-valerolactone with several different reaction temperatures. Tetrahydro-2-Furoic Acid in THP Reaction Time: 4 hr Catalyst: Reactant= 1:4 GC-MS results.

Since it had been determined that the catalyst can produce δ-valerolactone, the next step was to look at improving reaction conditions such as time and temperature to see their effects. Temperature effects were investigated by running several different reactions at temperatures from 80-180 °C. From the results shown in Figure 4.7, the production of δ-valerolactone peaks at around 100 °C and then quickly drops off. At temperatures below 100 °C the temperature is not high enough to overcome the activation barrier for the ring rearrangement reaction. Additionally, if the temperature exceeds 100 °C, the δ-valerolactone begins to degrade, suggesting that an additional reaction barrier has been overcome. Based on these results, the reaction temperature of 120 °C used previously should be reduced to 100 °C to maximize δ-

valerolactone production. This however does not explain why the final product was not produced previously as there is still a significant amount of δ-valerolactone at the higher reaction temperature used previously.

4.2.2.3 Reaction Time and Catalyst Deactivation

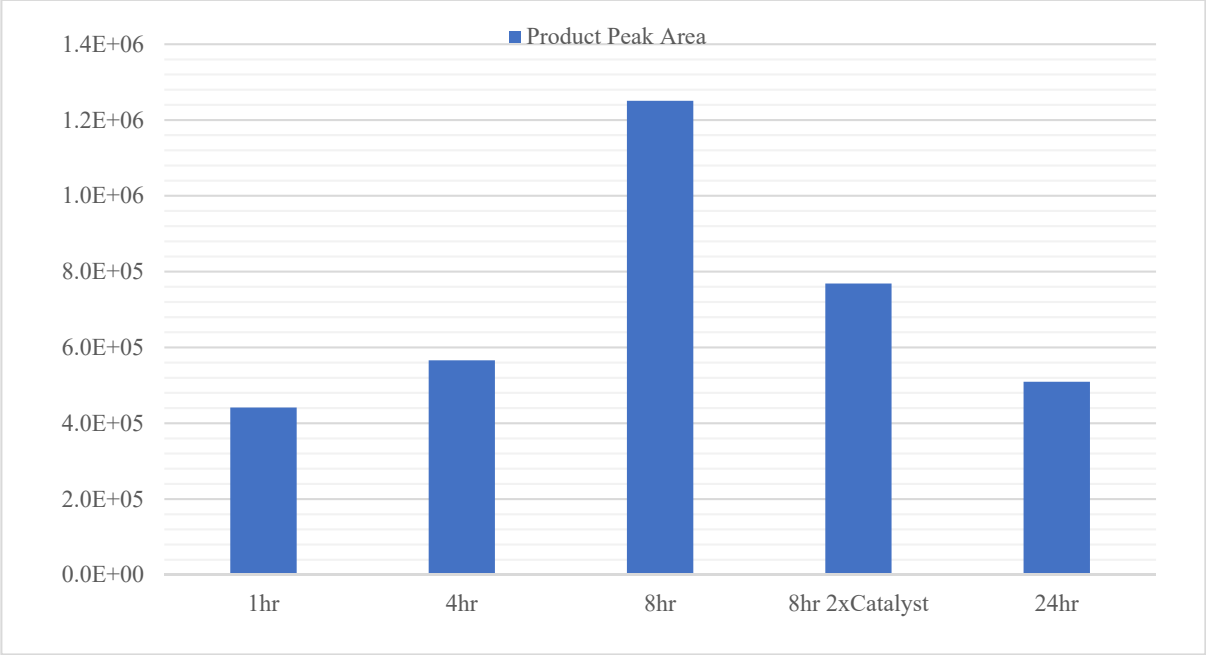

Figure 4.8: Reaction Time. Peak area for δ-valerolactone with several different reaction times. Tetrahydro-2-Furoic Acid in THP Catalyst= Pd sub BEA Catalyst:Reactant= 1:4 Temperature= 100 °C.

Reaction time was investigated by performing reactions starting with tetrahydrofuroic acid and varying the time from 1-24 hours. This work was to ensure that the reaction time was sufficient to produce δ-valerolactone as well as determining if the reaction time used previously was too long and product had the opportunity to degrade. From Figure 4.8 it can be see that the 8-hour reaction time proved to be the most effective. This shows that the reaction takes more time to produce the maximum amount of product than the 4 hours previously allotted and if it is left beyond 8 hours the product will degrade. To check for catalyst deactivation a second 8-hour reaction was conducted where after 4 hours more catalyst was added to the reactor and then the reaction continued for an additional 4 hours. If the catalyst had deactivated we would expect to

see more product formed whereas, above it can be seen less product was ultimately. From these results, it seems that the additional catalyst enabled the product to degrade into unwanted byproducts. Thus, it could be possible that the active sites needed for the degradation reactions may undergo a deactivation but through the addition of more catalyst the number of these active sites is revitalized allowing for more product degradation.

4.2.2.4 Hydrogen Pressure Effect

With these improved conditions, a reaction was run in a Parr reactor pressurized with hydrogen starting with 2-furoic acid this time at a temperature of 100 °C and a reaction time of 8 hours with the same weight ratios as before. This results from this setup showed that although the intermediate product, tetrahydro-2-furoic acid, was produced no δ-valerolactone was produced. A second reaction starting from tetrahydro-2-furoic acid was run with similar results. These outcomes demonstrate that the third and fourth reactions cannot both be completed with pressurized hydrogen. Although it has not been performed it is suspected that the fourth reaction were performed under the pressure of an inert gas the reaction would still occur. One hypothesis for the effect of the hydrogen reaction conditions comes from the work performed by Chia et. al. where a bifunctional Rh-ReO_x/C catalyst was used for hydrogenolysis of several oxygen containing hydrocarbons, mentioned previously.[26] In their study, they were looking to form long diol chains and were performing the reactions in flowing hydrogen. For this study, we seek to hydrogenate other bonds and form a six-membered ring so perhaps the additional hydrogen prevents the six-membered from forming and perhaps forming the diol in Figure 4.9. Another possibility is the carboxylic acid chain intermediate product in the same figure where perhaps the step to convert to the final lactone is not favored. Peaks for additional products were not examined so their existence is purely hypothetical at this point. An alternative explanation

would be that with the low conversion of reactant the amount of the lactone produced is no sufficient to produce a separate peak. In either case a more accurate analysis with quantification would need to be performed.

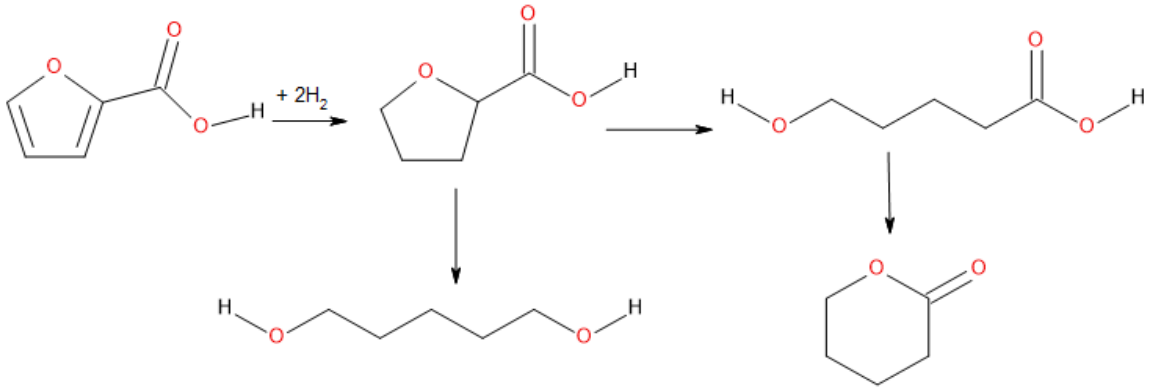

Figure 4.9: Alternative Products for Hydrogenation and Ring Rearrangement.

4.3 Conclusion

From the initial experiments, it was found that the secondary product, δ-valerolactone, could not be produced under the conditions needed for the hydrogenation. Upon further investigation in small batch reactors it was found that a lower reaction temperature of 100°C rather than 120°C would favor production of δ-valerolactone without allowing it to form as many unwanted byproducts. With this more suitable temperature the reaction time was then investigated trying reactions between 1-24 hours. For this it was found that a reaction time of 8 hours yielded the most product and reaction times beyond this allowed for the product to degrade. Similarly, if more catalyst was added at the 4-hour mark than the product would react away suggesting that the reaction was not involved in an equilibrium but rather the production was restricted by the formation of unwanted byproducts. Despite the difference in reaction conditions needed for both reactions it was found that both the hydrogenation and ring-rearrangement reactions can be performed using Pd/BEA. The Pd is the metal which saturates the ring while the zeolite provides the acid site which cleaves the C-O bond of the more substituted carbon. From these results, it

was determined that the ring opening reaction needs to take place in other, non-hydrogen pressurized conditions possibly due to a hydrogenation which prevents the formation of the six-membered ring. This would need to be further investigated by looking specifically to see if what byproducts are. In addition, to further validate these results a bi-substituted ring more similar to the molecules in the reaction scheme would need to be tested. This would add further complications, because in a ring like this there would be two points with similarly substituted carbons in C-O bonds. In summary, the first reaction occurs readily at 120 °C for 4 hours when pressurized to 500 psi with hydrogen. The second part of this reaction seems to be more productive at 100 °C and 8 hours without hydrogen with longer reaction time, higher temperature, and additional catalyst all causing degradation of product.

5. OUTLOOK AND FUTURE DIRECTIONS

5.1 Outlook

The work done here is a great step toward converting HMF into a tunable polymer. With the etherification reaction, it was determined that BEA-25 was the most effective catalyst. This was determined due to both its high selectivity as well as its high rate of ether production. This catalyst possesses the Brønsted sites needed for this reaction and contains them in such a way that the cage seems to help stabilize a protonated transition state that resembles HMF. Upon further study, it was found that because of this mechanism when different alcohols were used to react with HMF there appeared to be no effect on the amount of ether product formed. With the hydrogenation and ring rearrangement reaction it was found that Pd/BEA was a catalyst capable of performing both reaction steps. The other conditions needed however were different. For the hydrogenation step a 120 °C reaction for 4 hours with 500 psi of hydrogen was able to readily produce the saturated ring product. However, for the ring rearrangement product it was found that a lower temperature of 100 °C as well as a longer reaction time of 8 hours proved better for producing a six-membered lactone ring and was not productive if the system was pressurized with hydrogen. Overall, this study covers the first, third, and fourth reactions but, there are still more steps that need to be completed. Some of the future work that should be undertaken is included in this chapter.

5.2 Future Directions

5.2.1 Hydrogenation and Ring Rearrangement

As of this point the reactions have only been performed with simplified molecules in which only mono-substituted rings have been used. This is a good start to prove a mechanism, but further work should be done on bi-substituted and actual reaction molecules to verify that the

reaction conditions as well as the catalysts work for more complicated molecules. This is especially important as the reaction mechanism for the ring rearrangement reaction must take place at the correct C-O bond and with two equally substituted carbons adjacent to the furanic oxygen there are two places where the ring could open. Once this has been completed the two reactions could be linked together to see if the catalyst could be used without reactivation to perform both reactions by just relieving the hydrogen pressure in between.

5.2.2 Remaining Reactions

The main reaction left at this point is the second reaction, the oxidation. Although this reaction is well documented in the literature, the molecules used are different and so the catalyst and reaction conditions must be established for this reaction too. Based on the work done by Davis *et al.*, gold supported on either carbon or titanium oxide would work best to create the oxidation product for this reaction.[28] This reaction seems straight forward, so complications are not anticipated.

5.2.3 Full Reaction Scheme

Once all the individual reactions have been established all the reactions need to be performed subsequently to ensure that the full reaction scheme is an effective way to produce a tunable polymer from 5-hydroxymethylfurfural. Fluidity between the multiple steps for different solvents, separation procedures to get rid of excess alcohol in the first step for example, as well as the side products need to be determined. Some potential separation procedures to go along with these lab-scale reactions might include evaporation, use of drying agents such as sodium sulfate, or filtering for catalyst recovery.

5.2.4 HMF Source

Another important consideration for this work includes the use of HMF from a source which is not pure. As of this point in the work, the HMF used has come from a laboratory chemical supplier and as such does not come with the impurities one might expect from a direct biomass product. For example when HMF was produced from rice straw the material starts off with xylan, glucan, as well as lignin which results in the formation of HMF as well as other furan products.[29] This investigation would further determine if the scheme would still be effective with a cheaper, less refined source.

REFERENCES

(1) Ahn, Y.; Lee, S. H.; Kim, H. J.; Yang, Y.-H.; Hong, J. H.; Kim, Y.-H.; Kim, H. Electrospinning of Lignocellulosic Biomass Using Ionic Liquid. *Carbohydr. Polym.* **2012**, *88* (1), 395–398 DOI: 10.1016/j.carbpol.2011.12.016.

(2) Taherzadeh, M. J.; Karimi, K. *Pretreatment of Lignocellulosic Wastes to Improve Ethanol and Biogas Production: A Review*; 2008; Vol. 9.

(3) Huber, G. W.; Sara, I.; Corma, A. Synthesis of Transportation Fuels from Biomass. *Chem Rev.* **2006**, *2* (106), 4044–4098 DOI: 10.1021/cr068360d.

(4) U.S. Energy Information Administration. Independent Statistics and Analysis https://www.eia.gov/ (accessed Jul 17, 2017).

(5) Schwartz, T. J.; Shanks, B. H.; Dumesic, J. A. Coupling Chemical and Biological Catalysis: A Flexible Paradigm for Producing Biorenewable Chemicals.

(6) Siirola, J. J. The Impact of Shale Gas in the Chemical Industry. *AIChE* **2014**, *60* (3), 810–819 DOI: 10.1002/aic.

(7) Isikgor, F. H.; C. Remzi Becer. Lignocellulosic Biomass: A Sustainable Platform for Production of Bio-Based Chemicals and Polymers. *Polym. Chem.* **2015**, *6*, 4497–4559 DOI: 10.1039/c3py00085k.

(8) Marketsandmarkets.com. Lactic Acid Market by Application (Biodegradable Polymer, Food & Beverage, Personal Care & Pharmaceutical) & Polylactic Acid Market by Application (Packaging, Agriculture, Automobile, Electronics, Textile), & by Geography - Global Trends & Forecasts to 20 http://www.marketsandmarkets.com/Market-Reports/polylacticacid-387.html (accessed Jul 17, 2017).

(9) Lim, L.-T.; Auras, R.; Rubino, M. Processing Technologies for Poly(lactic Acid). *Prog. Polym. Sci.* **2008**, *33* (8), 820–852 DOI: 10.1016/j.progpolymsci.2008.05.004.

(10) Werpy, T.; Petersen, G. Top Value Added Chemicals from Biomass Volume I — Results of Screening for Potential Candidates from Sugars and Synthesis Gas Top Value Added Chemicals From Biomass Volume I : Results of Screening for Potential Candidates. *Other Inf. PBD 1 Aug 2004* **2004**, Medium: ED; Size: 76 pp. pages DOI: 10.2172/15008859.

(11) Saha, B.; Abu-Omar, M. M. Advances in 5-Hydroxymethylfurfural Production from Biomass in Biphasic Solvents. *Green Chem.* **2014**, *16* (1), 24 DOI: 10.1039/c3gc41324a.

(12) Tong, X.; Li, Y. Efficient and Selective Dehydration of Fructose to 5-Hydroxymethylfurfural Catalyzed by Brønsted-Acidic Ionic Liquids. *ChemSusChem* **2010**, *3* (3), 350–355 DOI: 10.1002/cssc.200900224.

(13) Carniti, P.; Gervasini, A.; Biella, S.; Auroux, A. Niobic Acid and Niobium Phosphate as Highly Acidic Viable Catalysts in Aqueous Medium: Fructose Dehydration Reaction. *Catal. Today* **2006**, *118* (3–4 SPEC. ISS.), 373–378 DOI: 10.1016/j.cattod.2006.07.024.

(14) Schwartz, T. J.; Bond, J. A Thermodynamic and Kinetic Analysis of Solvent-Enhanced Selectivity in Monophasic and Biphasic Reactor Systems. *Chem. Commun.* **2017**, *53*, 8148–8151 DOI: 10.1039/C7CC03164E.

(15) Román-Leshkov, Y.; Dumesic, J. A. Solvent Effects on Fructose Dehydration to 5-Hydroxymethylfurfural in Biphasic Systems Saturated with Inorganic Salts. *Top. Catal.* **2009**, *52* (3), 297–303 DOI: 10.1007/s11244-008-9166-0.

(16) Davis, S. E.; Houk, L. R.; Tamargo, E. C.; Datye, A. K.; Davis, R. J. Oxidation of 5-Hydroxymethylfurfural over Supported Pt, Pd and Au Catalysts. *Catal. Today* **2011**, *160* (1), 55–60 DOI: 10.1016/j.cattod.2010.06.004.

(17) Gallastegi-Villa, M.; Aranzabal, A.; González-Marcos, J. A.; González-Velasco, J. R. Metal-Loaded ZSM5 Zeolites for Catalytic Purification of Dioxin/furans and NOx Containing Exhaust Gases from MWI Plants: Effect of Different Metal Cations. *Appl. Catal. B Environ.* **2016**, *184*, 238–245 DOI: 10.1016/j.apcatb.2015.11.006.

(18) Lew, C. M.; Rajabbeigi, N.; Tsapatsis, M. One-Pot Synthesis of 5-(Ethoxymethyl)furfural from Glucose Using Sn-BEA and Amberlyst Catalysts. *Ind. Eng. Chem. Res.* **2012**, *51* (14), 5364–5366 DOI: 10.1021/ie2025536.

(19) Lanzafame, P.; Temi, D. M.; Perathoner, S.; Centi, G.; MacArio, A.; Aloise, A.; Giordano, G. Etherification of 5-Hydroxymethyl-2-Furfural (HMF) with Ethanol to Biodiesel Components Using Mesoporous Solid Acidic Catalysts. *Catal. Today* **2011**, *175* (1), 435–441 DOI: 10.1016/j.cattod.2011.05.008.

(20) Salminen, E.; Kumar, N.; Virtanen, P.; Tenho, M.; Mäki-Arvela, P.; Mikkola, J. P. Etherification of 5-Hydroxymethylfurfural to a Biodiesel Component over Ionic Liquid Modified Zeolites. *Top. Catal.* **2013**, *56* (9–10), 765–769 DOI: 10.1007/s11244-013-0035-0.

(21) Balakrishnan, M.; Sacia, E. R.; Bell, A. T. Etherification and Reductive Etherification of 5-(Hydroxymethyl)furfural: 5-(Alkoxymethyl)furfurals and 2,5-Bis(alkoxymethyl)furans as Potential Bio-Diesel Candidates. *Green Chem.* **2012**, *14* (6), 1626–1634 DOI: 10.1039/C2GC35102A.

(22) Mellmer, M. A.; Gallo, J. M. R.; Martin Alonso, D.; Dumesic, J. A. Selective Production of Levulinic Acid from Furfuryl Alcohol in THF Solvent Systems over H-ZSM-5. *ACS Catal.* **2015**, *5* (6), 3354–3359 DOI: 10.1021/acscatal.5b00274.

(23) Sarazen, M.; Doskocil, E.; Iglesia, E. The Effects of Void Environment and Acid Strength on Alkene Oligomerization Selectivity. *ACS Catal.* **2016**, *6*, 7059–7070 DOI: 10.1021/acscatal.6b02128.

(24) Frillette, V. J.; Haag, W. O.; Lago, R. M. Catalysis by Crystalline Aluminosilicates: Characterization of Intermediate Pore-Size Zeolites by the "Constraint Index." *J. Catal.* **1981**, *67* (1), 218–222 DOI: 10.1016/0021-9517(81)90273-6.

(25) Jae, J.; Tompsett, G. A.; Foster, A. J.; Hammond, K. D.; Auerbach, S. M.; Lobo, R. F.; Huber, G. W. Investigation into the Shape Selectivity of Zeolite Catalysts for Biomass Conversion. *J. Catal.* **2011**, *279* (2), 257–268 DOI: 10.1016/j.jcat.2011.01.019.

(26) Chia, M.; Pagán-Torres, Y. J.; Hibbitts, D.; Tan, Q.; Pham, H. N.; Datye, A. K.; Neurock, M.; Davis, R. J.; Dumesic, J. a. Selective Hydrogenolysis of Polyols and Cyclic Ethers over Bifunctional Surface Sites on Rhodium-Rhenium Catalysts. *J. Am. Chem. Soc.* **2011**, *133* (32), 12675–12689 DOI: 10.1021/ja2038358.

(27) Chia, M.; O'Neill, B. J.; Alamillo, R.; Dietrich, P. J.; Ribeiro, F. H.; Miller, J. T.; Dumesic, J. A. Bimetallic RhRe/C Catalysts for the Production of Biomass-Derived Chemicals. *J. Catal.* **2013**, *308*, 226–236 DOI: 10.1016/j.jcat.2013.08.008.

(28) Davis, S. E.; Benavidez, A. D.; Gosselink, R. W.; Bitter, J. H.; De Jong, K. P.; Datye, A. K.; Davis, R. J. Kinetics and Mechanism of 5-Hydroxymethylfurfural Oxidation and Their Implications for Catalyst Development. *J. Mol. Catal. A Chem.* **2014**, *388–389*, 123–132 DOI: 10.1016/j.molcata.2013.09.013.

(29) Amiri, H.; Karimi, K.; Roodpeyma, S. Production of Furans from Rice Straw by Single-Phase and Biphasic Systems. *Carbohydr. Res.* **2010**, *345* (15), 2133–2138 DOI: 10.1016/j.carres.2010.07.032.

(30) Princeton. Zeomics http://helios.princeton.edu/zeomics/ (accessed Jul 19, 2017).

(31) IZA Structure Commision. IZA Structure Commission http://www.iza-structure.org/ (accessed Jul 19, 2017).

BIOGRAPHY OF THE AUTHOR

Meredith C. Allen was born in Farmington, Maine on May 13th, 1991. She grew up in Farmington and graduated from Mt. Blue High School in 2009. She attended St. Lawrence University in Canton, New York and graduated with a Bachelor of Science degree in chemistry and a minor in mathematics in 2013. After this, she worked from 2013-2015 as a chemistry analyst at Northeast Laboratory Services in Winslow, Maine. She then entered the Chemical Engineering graduate program at the University of Maine in the fall of 2015. She is a candidate for the Master of Science degree in Chemical Engineering from the University of Maine in August 2017.